Title: **Mesoscale eddies regulate seasonal iron supply and carbon drawdown in the Drake Passage**

Authors: Annika Jersild*, Sara Delawalla, and Takamitsu Ito

Affiliation: School of Earth and Atmospheric Sciences, Georgia Institute of Technology, Atlanta Georgia, USA

Corresponding author: Annika Jersild (Email: ajersild3@gatech.edu)

Key Points:

- Resolving mesoscale ocean eddies is critical for the seasonality of the regional carbon cycle in the Drake Passage.
- Eddy parameterization reduces the annual mean carbon cycle bias but does not improve the seasonal cycle
- Suppressing eddy activity increases iron supply, causing a stronger and earlier spring bloom at the expense of summer-time productivity

Abstract

The Southern Ocean is a major region for uptake of anthropogenic carbon. The transport of carbon and nutrients are dominated by the Antarctic Circumpolar Current and its rich mesoscale eddy field, however, current generation of Earth System Models lack the resolution to resolve eddies. Here we show that a computational model that explicitly represents mesoscale eddies can reproduce observed phases and amplitudes of seasonal biological productivity and partial pressure of carbon dioxide. Our sensitivity study demonstrates that when eddies are suppressed or parameterized, the model cannot reproduce these seasonal cycles. Experiments with suppressed eddy activity show that the lack of eddies significantly changes the iron supply and phenology of phytoplankton blooms. The mismatch in the timing and intensity of the bloom causes significant biases in the seasonal carbon cycle of the region with implications to the enigmatic biases in partial pressure of carbon dioxide among the state-of-the-art Earth System Models.

Plain Language Summary

The Southern Ocean plays a critical role in the global carbon cycle and is an important region for uptake of carbon. Movement of carbon and nutrients in this region is driven by lots of smaller scale (10-100km) transient movements, known as mesoscale eddies. We use a computational model to run a sensitivity study analyzing the impact of these movements on the seasonality of surface carbon in the Drake Passage region. We find that when the mesoscale eddies are explicitly represented, we are able to reproduce the seasonal cycle of carbon dioxide and biological productivity. However, when the small-scale movements are suppressed or represented through a parameterized equation, the model cannot reproduce the seasonality. Model runs that suppress the transient movements shift the surface iron supply and result in a change of timing and intensity of summertime phytoplankton blooms, which causes bias in the seasonal carbon cycle. This research has important implications for modeling, parameterization, and resolution choices when looking at questions relying on the seasonal-scale of the carbon cycle.

1. Introduction

The Southern Ocean plays a critical role in the global carbon cycle. The dominating current in the region, the Antarctic Circumpolar Current (ACC), circumnavigates the globe and connects all of the major ocean basins. Its overturning circulation brings up the deep water and subducts thermocline and intermediate waters that are major conduits for the oceanic uptake of heat and anthropogenic carbon (Armour, Marshall, Scott, Donohoe, & Newsom, 2016; Ben Bronselaer & Zanna, 2020; Toggweiler & Russell, 2008), contributing over 40 percent of the ocean carbon uptake (Khatiwala, Primeau, & Hall, 2009). Despite its importance, there are large uncertainties surrounding components controlling the regional carbon flux. While the state-of-the-art Earth System Models (ESMs) generally reproduce the annual mean carbon flux in the region, its seasonal cycle is often poorly correlated with observations (Jiang, Gille, Sprintall, & Sweeney, 2014; Mongwe, Chang, & Monteiro, 2016).

The ACC is filled with mesoscale (approx. 10-100km) features with meandering jets and vortices (eddies) that play central roles to maintain the stratification and the overturning circulation with global implications (Gnanadesikan, 1999; Johnson & Bryden, 1989; Marshall & Radko, 2003; Marshall & Speer, 2012). This rich mesoscale eddy field is critical for the transport of carbon and nutrients in the region, but the current generation of ESMs cannot resolve these features due to their coarse resolution and the eddies are challenging to parameterize realistically.

In order to study the influence of mesoscale eddies on the carbon cycle in this region, we perform and compare three computational simulations for a sensitivity study using a regional physical and biological model with a 10-km horizontal resolution. This modeling study is focused on the Drake Passage region, which is the only section of the Antarctic Circumpolar

Current (ACC) bounded by land topography to the north and south and relatively well sampled by ship-based observations. The three runs compare the same region with resolved mesoscale eddies, parameterized mesoscale eddies, and eddies suppressed via enhanced viscous friction. We compare the surface partial pressure of carbon dioxide (pCO_2) and the seasonal carbon and iron budgets to show the importance of resolving mesoscale eddies for reproducing seasonality in the Drake Passage region.

2. Model configurations and experimental design

The regional physical and biological model for the Drake Passage region is simulated in three configurations, "Control", "No Eddy", and "GM/Redi". The control simulation follows the work of Jersild and Ito (Jersild & Ito, 2020), where the model domain covers from 80°W to 40°W and from 70°S to 45°S. The Control run includes biharmonic viscosity for momentum and biharmonic diffusion for tracers both set to $3x10^9$ m^4/s (comparable to 30 m^2/s for Laplacian viscosity/diffusivity). The "No Eddy" simulation follows the same configuration but additional horizontal (Laplacian) viscosity is included at 1000 m^2/s, suppressing eddies, while tracer diffusivity is not altered. The "GM/Redi" simulation is the same, but eddies are parameterized by the isopycnal thickness and tracer diffusion scheme (Gent & Mcwilliams, 1990; Redi, 1982). The GM scheme represents the advective effect of mesoscale eddies that tends to flatten isopycnal surfaces, and the Redi scheme represents the diffusive effect by mixing tracers along isopycnal surfaces. Thus, the GM/Redi is expected to produce more stratified and well mixed properties relative to the No Eddy run. For simplicity, uniform constant GM coefficient and isopycnal diffusivity are used at the rate of 1000 m^2/s, which is set equal to the elevated viscosity.

For all three simulations, the hydrodynamics is based on Navier-Stokes equation in hydrostatic and Boussinesq approximation, and the domain is discretized into a longitude-latitude grid at a nominal 10-km resolution with 42 vertical depth levels. Grid spacing is approximately 10m near the surface and increases to 250m at the bottom (5500m). The model has open boundary conditions on all four sides which are restored to the data-constrained circulation and biogeochemical fields of the Biogeochemical Southern Ocean State Estimate ensuring the realistic boundary properties (B-SOSE, (Verdy & Mazloff, 2017)). Surface momentum and buoyancy forcing is taken from NCEP-2 reanalysis products at daily frequency (Kanamitsu et al., 2002) and the surface temperature and salinity fields are weakly restored towards B-SOSE climatology to minimize model drift.

The biological and biogeochemical components of the model are based on the 6 phytoplankton version of the Darwin model (Dutkiewicz et al., 2015) with improved representation of iron biogeochemistry including three classes of iron-binding ligands, sedimentary and hydrothermal iron sources, and interactions between particulate and dissolved iron (Pham & Ito, 2021). Furthermore, this model represents the iron limitation on the photosynthetic efficiency and the variable iron to carbon ratio in the biological parameterizations.

3. Results

3.1 An overview of the sensitivity experiments

The three simulations, “Control”, “No Eddy”, and “GM/Redi”, exhibit large differences in patterns of both horizontal and vertical distribution of tracers (Figure 1). Detailed analysis has been completed on a central, non-coastal region bounded by 57-60°S and 55-65°W, denoted by the boxes in the top row of Figure 1. As expected, surface current speed is diminished in the No Eddy and GM/Redi runs due to the elevated level of viscous friction. The hydrographic structure is altered in the sensitivity experiments. The Control run exhibits flatter isopycnals and cooler temperatures in the thermocline of the central Drake Passage region and a steep (nearly vertical) isopycnal slope associated with the narrow jet at the northern shelf break. The No Eddy and GM/Redi runs show warmer thermocline in the central Drake Passage with more gradual change in temperature. The average mixed layer depths (MLD) are generally similar between the three runs, 104m for the Control, 94m for the No Eddy, and 112m for the GM/Redi run, but the GM/Redi run does not represent the subsurface temperature minima that are present in the Control and the No Eddy runs. Stronger differences in MLD are found on seasonal timescale, but no coherent patterns are found. MLD is comparable across all three runs for the first year, year two the GM/Redi run has a deeper wintertime MLD, and year five the control run has the deepest MLD, with all three returning to the same summertime depth averaging around 50m (Supplementary Figure 1). These variations in seasonal pattern provide motivation for diving deeper into the other ways mesoscale eddies influence the near-surface carbon cycle.

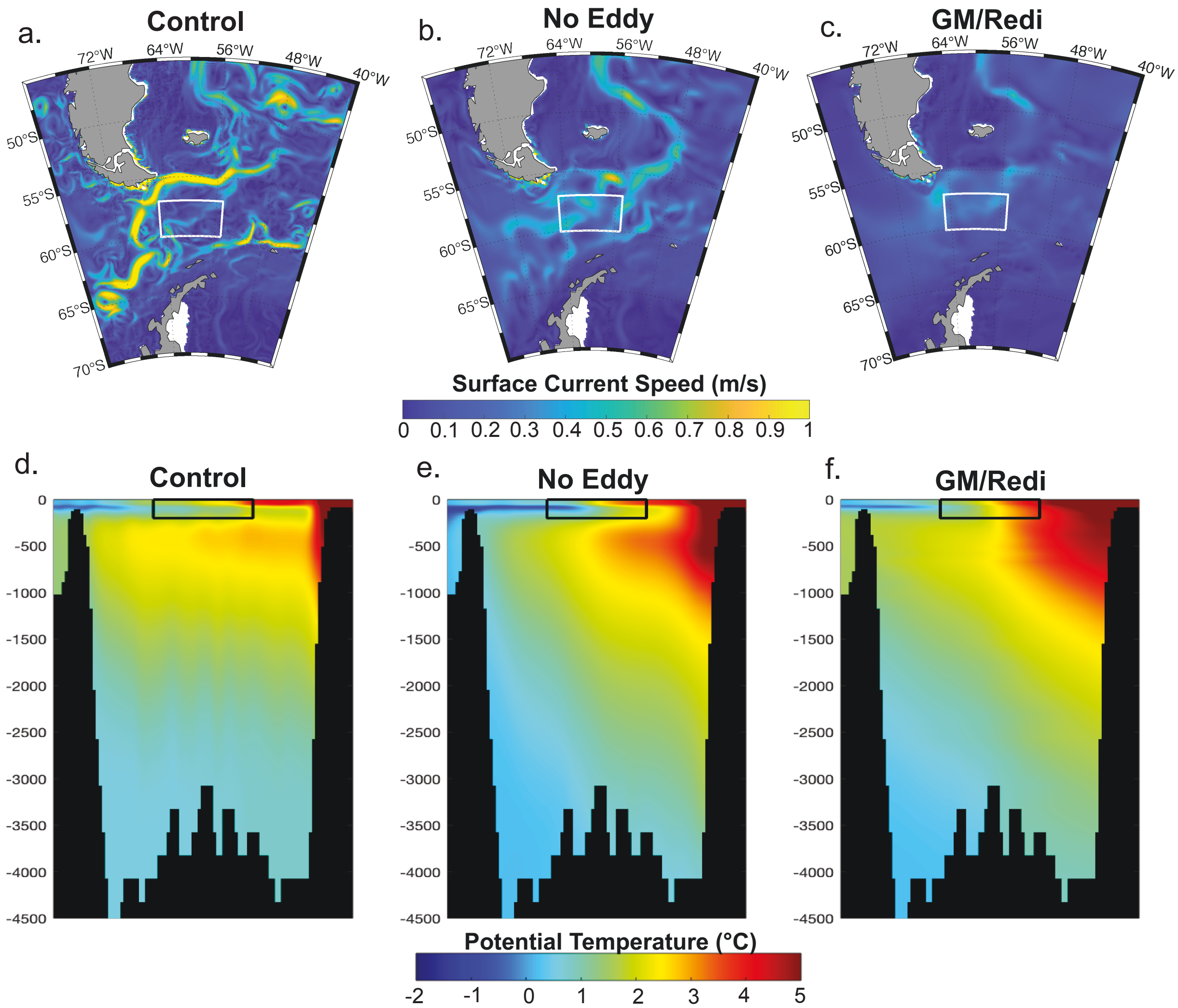

Figure 1. Comparison of Control run on left (a,d), No Eddy run in the middle (b,e) and GM/Redi run on the right (c,f) for July surface current speed (a,b,c) and vertical transect of potential temperature at 65°W (d,e,f).

3.2 Drivers of partial pressure of CO_2

The modeled surface partial pressure of Carbon Dioxide (pCO_2) is compared to the observationally derived pCO_2 product from Landschützer et al (Landschutzer, Gruber, & Bakker, 2020) (hereafter L20) for both mean bias and temporal correlation (Figure 2). These metrics are calculated using the model output interpolated onto 1° x 1° monthly grid points of the L20 product which uses a machine learning approach to fill data gaps for the open ocean observations excluding coastal oceans. Because potentially significant biases are expected in the coastal waters along the shelves of the South America and Antarctic continents, the comparisons are performed for the open ocean only. The control run is overall negatively biased (-8.4 ppmv) with a positive correlation throughout most of the domain (r=0.71) in the central Drake Passage region, whereas the No Eddy run exhibits opposite signals in the western and eastern portions of the domain with a smaller mean bias (Figure 2b, -1.5 ppmv). The No Eddy run has negative temporal correlation with the observation (r=-0.2). While the GM/Redi run does improve the annual patterns and the mean bias (Figure 2c, -2.0 ppmv), when the temporal correlation is compared, the GM/Redi run does not robustly reproduce observations (Figure 2g, r=-0.02). While all three runs captured the annual mean pCO_2 within observational uncertainty (approximately 12 ppmv (Landschutzer, Gruber, Bakker, & Schuster, 2014)), the Control run is significantly better than the other runs in reproducing the temporal evolution of the surface ocean pCO_2.

Additional observational product is incorporated from the SeaFlux ensemble which includes six observation-based pCO_2 products that regularly update and incorporate data from the SOCAT database, including the Landschützer data (Fay et al., 2021). To provide comparison to the neural-network derived product provided by Landschützer, we incorporate the JMA-MLR, a multiple linear regression, in Figure 2g.

In the center of the Drake Passage region (approximately 65°W, 58°S) the difference between the “Control”, “No Eddy”, and “GM/Redi” runs are small (Figure 2). All three simulations slightly underestimate surface ocean pCO_2 in the mean sense. The major difference occurs in the downstream of the ACC to the east of the Drake Passage (approximately 55°W, 55°S) where the control run shows slightly negative mean bias where the “No Eddy” run shows a much larger positive bias and the “GM/Redi” run shows a smaller positive bias. This bias becomes more pronounced towards the northeastern corner of the model domain. As stated earlier, the L14 dataset may not represent coastal waters well. The modeled coastal regions are highly productive and it tends to bring down surface ocean pCO_2 to a significantly lower value.

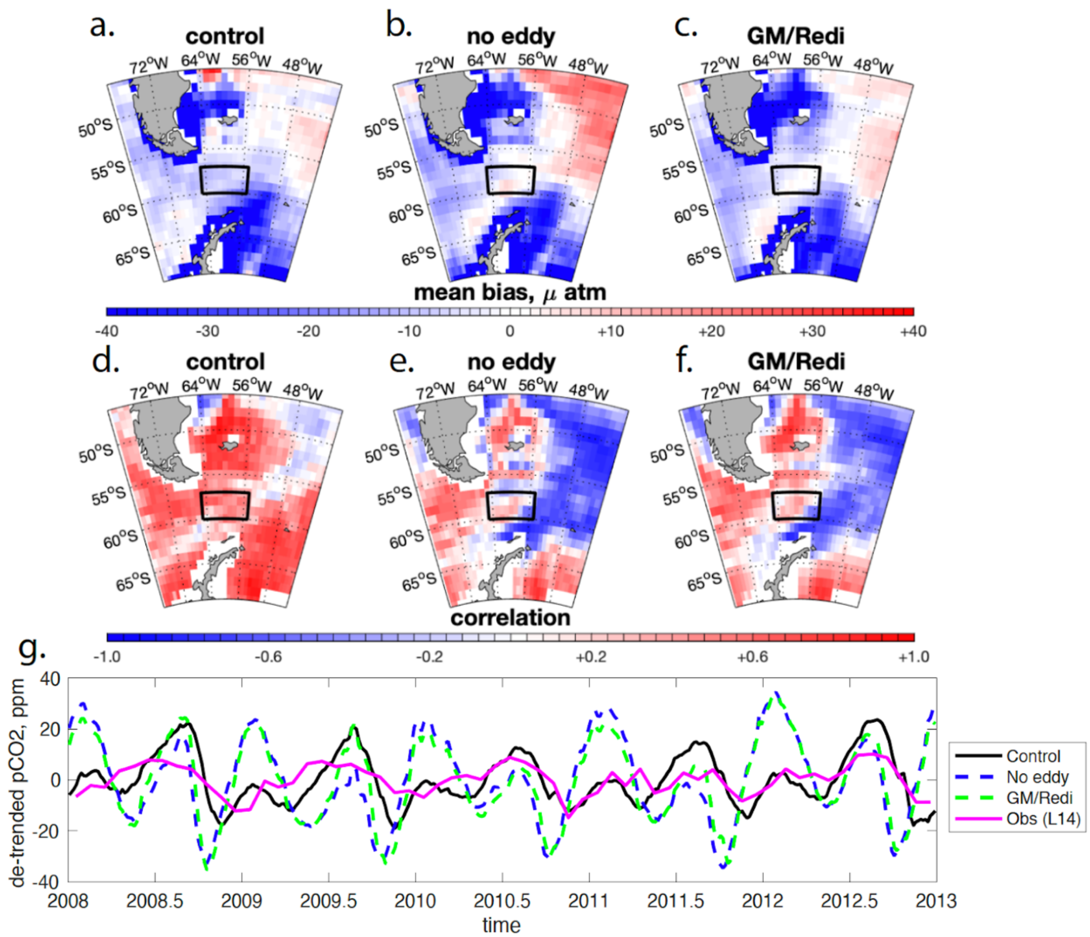

Figure 2. Evaluation of surface ocean pCO_2 in terms of (a-c) annual mean bias, (d-f) temporal correlation and (g) regionally averaged time series of central boxed region (57-60°S by 55-65°W). The three simulations (Control, No Eddy and GM/Redi) are compared against observation (Landschutzer et al., 2016) for the 5-year period of 2008-2012. Black dots in panel (d-f) indicate statistically significant correlation at 95% confidence level.

Figure 2 also compares the correlations between the model and observation (L14) for the three simulations (panel d, e and f). The effect of eddies is more obvious in this comparison. Overall modeled pCO_2 is strongly correlated with the observation when the effects of eddies are fully represented in the "Control" run (Fig 2d), however, a slightly negative correlation is found in the northeastern part of the domain. In the Drake Passage region (approximately 65°W, 58°S) the correlation is positive in the "Control" run but it is close to zero in the "No Eddy" and the "GM/Redi" runs (Fig 2ef). For all runs, the correlation values are lower in the eastern half of the domain. The "No Eddy" and "GM/Redi" runs have generally lower correlation and become negative in almost half of the domain.

The pCO_2 variability is driven by temperature, dissolved inorganic carbon (DIC), salinity, and alkalinity through equilibrium carbonate chemistry. In the Southern Ocean, the primary drivers are temperature and DIC with opposing effects on the seasonal cycles. During summers, elevated biological carbon uptake reduces the surface DIC and pCO_2, partially compensated by the lower solubility with warmer temperatures. In winters, entrainment of subsurface waters raises surface DIC and pCO_2, partially compensated by the higher solubility with cold temperatures. The net effect is dominated by the DIC changes in the Drake Passage region (Fay et al., 2018). Observations demonstrate a maximum in pCO_2 in winter months (July-September), and this feature is well represented by the output of the Control run (Figure 2g). In both the No Eddy and GM/Redi runs, there are strong peaks in late summer, driven by the warmer sea surface temperature (SST) and lower solubility, that do not agree with the observations. The summertime secondary peaks may be visible in the Control and observations but they are in much smaller amplitudes than the primary wintertime peaks. While the pCO_2 seasonal patterns vary significantly between the three runs, the temperature between these runs is comparable. All three runs exhibit similar seasonal patterns and no clear bias between the runs when compared across years (Supplementary Figure 2). Therefore, in order to further analyze the differences between the drivers of seasonal pCO_2, we turn to the DIC budget.

3.3 Dissolved Inorganic Carbon budget

The evolution of surface DIC is driven by fluxes due to air-sea gas exchange, evaporation-minus-precipitation, advection, mixing and biological sources and sinks (Figure 3a,b). The carbon budget is analyzed for the central Drake Passage region in the top 200m. The air-sea gas flux, a net positive source into the ocean, is a seasonal flux driven by the air-sea disequilibrium of pCO_2. Its uptake is strongest when the surface pCO_2 is at its minimum. Evaporation minus precipitation also occurs at the surface, and is a net negative flux in this region due to the net precipitation diluting DIC. While this is an apparent carbon sink, it has limited impact of ocean pCO_2 because it also dilutes the total alkalinity at the same rate. The (resolved) advection term is the convergence of advective carbon flux, including both the mean flow and the effect of transient eddies as resolved by the model velocity field. While it does not have a clear seasonal pattern, overall, it is a positive source of carbon in the surface region. The (parameterized) mixing term includes the background vertical diffusion, the horizontal biharmonic diffusion, and the vertical mixing due to the KPP parameterization (Large, McWilliams, & Doney, 1994). In the Control and No Eddy runs, the mixing term is dominated by the parameterized convection due to the KPP scheme. In the GM/Redi run, the effects of parameterized mixing are also included in this term, which explains the much larger contribution of the (parameterized) mixing term in the overall carbon budget relative to the Control and No Eddy runs for that component in Figure 3b.

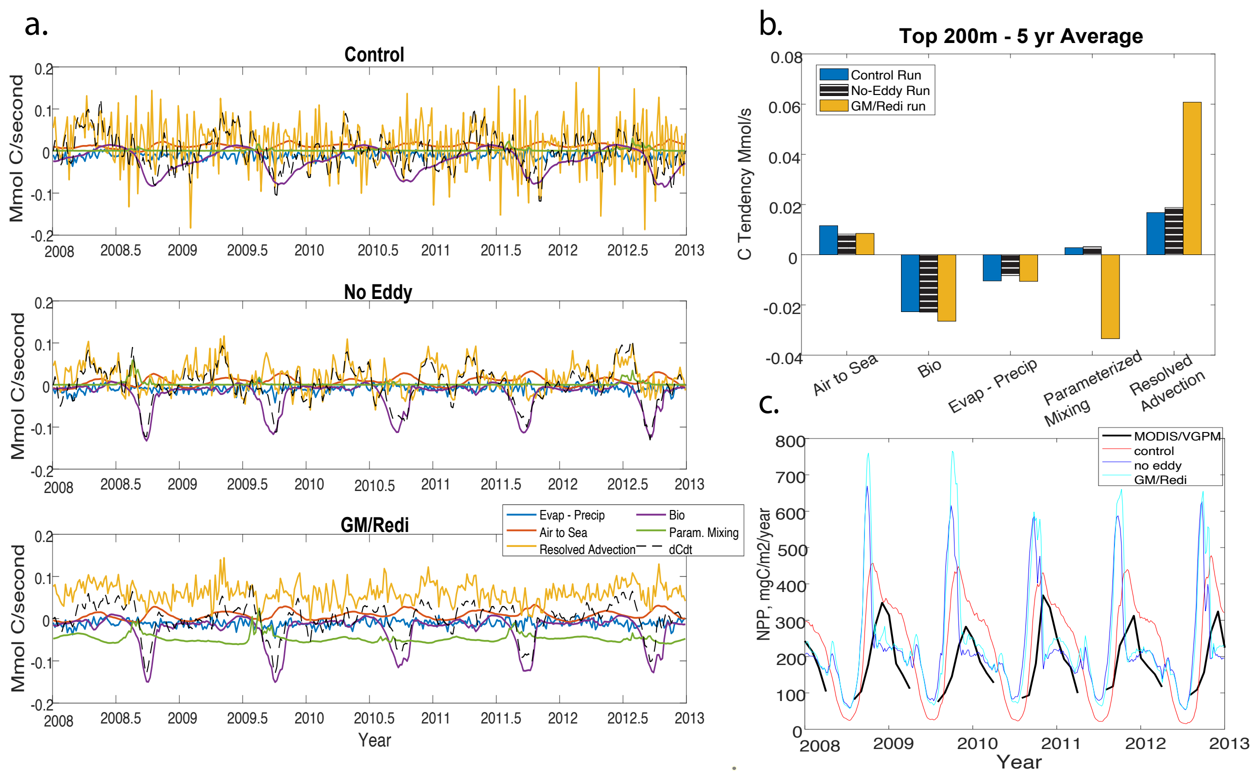

Figure 3. DIC budget terms, averaged over top 200m of central Drake Passage box (57-60°S by 55-65°W). (a) Time series from 2008-2012 showing magnitude and seasonality of components of the DIC budget including evaporation minus precipitation, air-to-sea flux, resolved advection, biological flux, and parameterized mixing for Control run (top), No Eddy run (middle), and GM/Redi run (bottom). (b) Bar plot showing magnitudes of flux averaged across 5 years, 2008-2012 for Control (blue), No-Eddy (black striped), and GM/Redi run (gold). (c) Net Primary Productivity (NPP) for each run compared with the MODIS/VGPM satellite data from 2008-2012.

4. Sensitivity of Biological Productivity and Iron Cycling

The biological processes influencing the surface DIC includes photosynthesis, remineralization of dissolved and particulate organic matter, and the dissolution and production of calcium carbonate. While the net biological carbon export are similar in terms of the magnitude for all three runs (Figure 3b), the amplitudes and patterns of seasonal cycle are significantly different between the three runs (Figure 3a). The biological carbon uptake of the Control run has a longer season of drawdown across the summertime months, whereas the runs without eddies have a very sharp, strong uptake that dies off quickly after the spring bloom. Evidence of the influence of this change in biological drawdown is exhibited in the net primary productivity (NPP), with a seasonal shift visible from a sharper peak and faster drawdown in the No Eddy and GM/Redi runs to a smaller peak and longer season of productivity across the summertime months in the Control run (Figure 3c). The seasonality of the Control run is a better representation of observations based on the satellite ocean color product (Behrenfeld & Falkowski, 1997).

While the seasonal sea surface temperature changes are important, the dominant driver of ocean pCO_2 in this region is the biological carbon uptake and export (Jersild & Ito, 2020).The productivity of the Southern Ocean is iron-limited. Deep wintertime mixing and diapnycal mixing are thought to be the dominating sources of dissolved iron to the surface ecosystem (Tagliabue, Williams, Rogan, Achterberg, & Boyd, 2014), and mesoscale eddies play a critical role in the productivity of the region (Ellwood et al., 2020). In order to analyze this shift in net primary productivity and biological drawdown, we compare the iron budget of the three runs (Figure 4). The iron budget is made up of many terms but can be categorized into five groups including (1) resolved advection, (2) parameterized mixing including wintertime mixing and GM/Redi parameterization, (3) biological uptake, (4) remineralization including the release from particulate phase (i.e. remineralization minus scavenging), and (5) external sources including dust, sedimentary and hydrothermal input. The sum of these five terms control the temporal evolution of dissolved iron field. This budget varies between all three runs for both seasonal patterns and annual averages (Figure 4ab).

The No Eddy and GM/Redi runs both have stronger physical iron supply by advection and parameterized mixing in the annual mean sense (Figure 4b), and as a consequence, these runs also show stronger biological drawdown of iron than in the Control run. This is caused by different transport terms (Figure S3). The mean upwelling is too strong in the No Eddy run, and the parameterized, winter-time mixing is too strong in the GM-Redi run. It is important to highlight the role of spring bloom in facilitating the stronger biological drawdown. These runs have the indication of the sharper peaks of the springtime, diatom-dominated bloom, likely caused by the stronger physical supply of iron. The oversupply of iron in these runs leads to a shift in phytoplankton community structure towards diatom dominance (Figure 4c). In this model, there are two major phytoplankton groups in the region, diatoms and picoplankton. Diatom quickly grows early in the season but it requires a higher level of iron supply, and it tends to die off once the iron level goes down in the summertime. In both the GM/Redi run and the No Eddy run, we see a shift to a stronger, earlier and sharper peak of diatoms correlated with a lower magnitude and a later bloom for the picoplankton.

The shift in community structure explains the pCO_2 seasonality of the region. In the Control run, diatom is still the major driver of biological carbon uptake but it is sustained by both diatom and picoplankton throughout the summer season, thus it maintains the surface pCO_2 level relatively low despite the warmer SST. By suppressing the eddies, those sensitivity runs enhanced the level of physical iron supply to the surface layer, intensifying the diatom bloom that shifted the seasonal cycle of surface pCO_2.

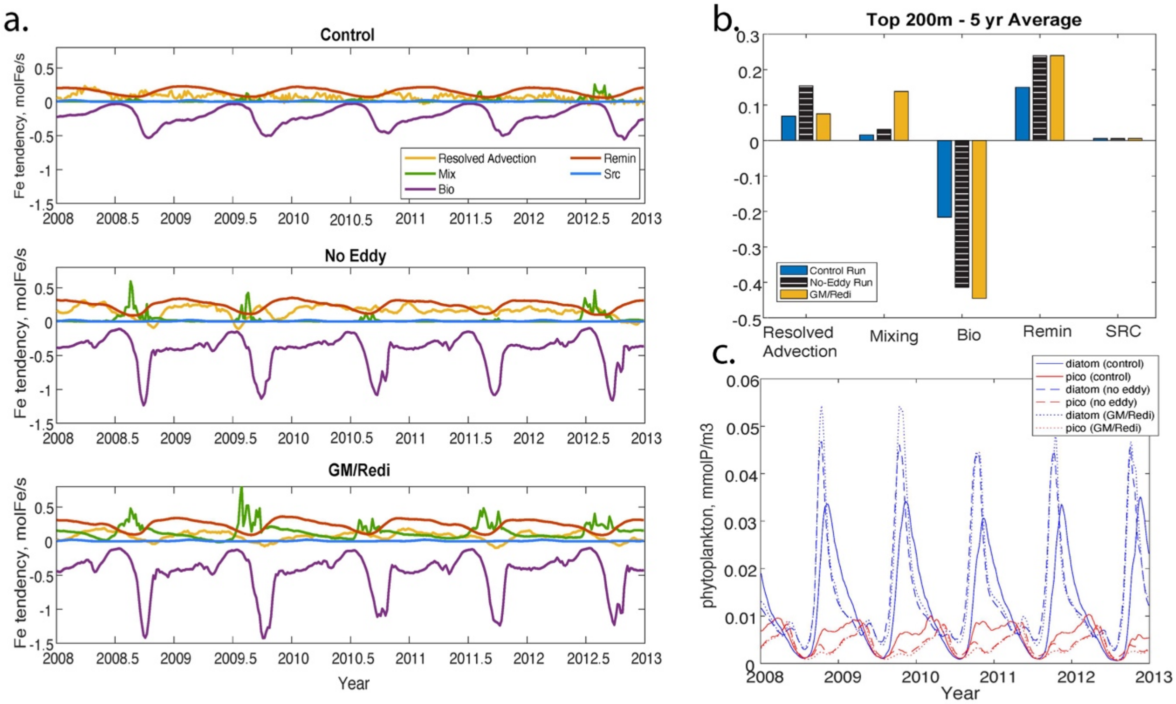

Figure 4. Breakdown of Iron budget, averaged over top 200m of Drake Passage central region (57-60°S by 55-65°W). (a) components of iron budget over time including resolved advection, mixing, biological flux, remineralization, and src (term including sedimentary iron input and hydrothermal iron), for Control run (top), No Eddy run (middle) and GM/Redi run (bottom). (b) bar plot showing magnitudes of flux averaged across 5 years, 2008-2012 for Control (blue), No-Eddy (black striped), and GM/Redi run (gold). (c) phytoplankton concentration for Control run (line), No Eddy run (dashed), and GM/Redi run (dotted) for the two dominating phytoplankton in the region, diatoms and picoplankton.

5. Conclusions

Resolving mesoscale eddies is critical for reproducing the seasonality of the carbon cycle in the Drake Passage. When mesoscale eddies are suppressed, the annual mean remains comparable especially when the GM/Redi parameterization is applied. The eddy parameterization indeed improves the pattern of annual mean pCO_2. However, the phases of the seasonal cycle did not show a similar improvement. The Control run better reproduces seasonality in the surface pCO_2, with a longer, sustained biologically-driven carbon flux that lasted further into the summer season. Suppressing the eddy activity led to an increase in the iron supply either through increased advection or eddy parameterization, and disrupted the summer-time productivity, which caused seasonal pCO_2 bias in our sensitivity study.

Our results have implications for the interpretation of current ESMs and their ability to reproduce the correct seasonal cycle of the carbon cycle in the Southern Ocean. Many ESMs include explicit representations of the phytoplankton community in the surface ocean but the mesoscale eddies still need to be parameterized for the long-term integrations on the relevant timescales concerning global climate change. For seasonality and shorter time scale, mesoscale eddies are critical and parameterization can still poorly reproduce the seasonal carbon flux. One caveat of this study is that the nominal 10km resolution cannot represent submesoscale eddies which can also plan an important role (Uchida et al., 2020). However, the comparability of the annual mean pCO_2 could have a certain level of confidence associated with the annual and long-term projections. It should also be noted that variations in choice of iron scheme can have a large influence on both seasonal iron supply and subsequent phytoplankton growth and ecosystem carbon (Pham & Ito, 2021). In this sensitivity study, since the same iron forcings were used across the runs, we attribute the differences in results to other components. However, the importance of iron scheme choice should be considered when applying these results to other regions or models.

This research serves as motivation for further regional high-resolution studies to investigate the role of mesoscale/submesoscale processes to better simulate and understand regional, seasonal-scale biogeochemical dynamics. Further sensitivity studies in other sectors of the Southern Ocean are warranted to apply the conclusions to a broader scale, with important implications for lower-resolution ESMs and mesoscale eddy parameterizations.

Acknowledgements

This study is supported by the U.S. National Science Foundation, OPP-1744755. Modifications to the MITgcm source code, scripts, and instructions to reproduce input files for the model simulations are available as the Regional Southern Ocean package (Version v1.0, Zenodo, https://doi.org/10.5281/zenodo.3754803).

References

Armour, K. C., Marshall, J., Scott, J. R., Donohoe, A., & Newsom, E. R. (2016). Southern Ocean warming delayed by circumpolar upwelling and equatorward transport, 1–7. http://doi.org/10.1038/ngeo2731

Behrenfeld, M. J., & Falkowski, P. G. (1997). Photosynthetic rates derived from satellite-based chlorophyll concentration. *Limnology and Oceanography*, *42*(1), 1–20. http://doi.org/10.4319/lo.1997.42.1.0001

Ben Bronselaer, & Zanna, L. (2020). Heat and carbon coupling reveals ocean warming due to circulation changes. *Nature*, 1–21. http://doi.org/10.1038/s41586-020-2573-5

Dutkiewicz, S., Hickman, A. E., Jahn, O., Gregg, W. W., Mouw, C. B., & Follows, M. J. (2015). Capturing optically important constituents and properties in a marine biogeochemical and ecosystem model. *Biogeosciences*, *12*(14), 4447–4481. http://doi.org/10.5194/bg-12-4447-2015

Ellwood, M. J., Strzepek, R. F., Strutton, P. G., Trull, T. W., Fourquez, M., & Boyd, P. W. (2020). Distinct iron cycling in a Southern Ocean eddy. *Nature Communications*, 1–8. http://doi.org/10.1038/s41467-020-14464-0

Fay, A. R., Gregor, L., Landschützer, P., McKinley, G. A., Gruber, N., Gehlen, M., et al. (2021). SeaFlux: harmonization of air–sea CO2 fluxes from surface pCO2 data products using a standardized approach. *Research-Collection.Ethz.Ch*. http://doi.org/10.5194/essd-2021-16

Fay, A. R., Lovenduski, N. S., McKinley, G. A., Munro, D. R., Sweeney, C., Gray, A. R., et al. (2018). Utilizing the Drake Passage Time-series to understand variability and change in subpolar Southern Ocean. *Biogeosciences*, *15*(12), 3841–3855. http://doi.org/10.5194/bg-15-3841-2018

Gent, P. R., & Mcwilliams, J. C. (1990). Isopycnal Mixing in Ocean Circulation Models. *Journal of Physical Oceanography*, *20*(1), 150–155. http://doi.org/10.1175/1520-0485(1990)020<0150:IMIOCM>2.0.CO;2

Gnanadesikan, A. (1999). A Simple Predictive Model for the Structure of the Oceanic Pycnocline. *Science*, *283*(5410), 2077–2079. http://doi.org/10.2307/2896696?refreqid=search-gateway:df43f1887aeb141c0728ac254be90ba8

Jersild, A., & Ito, T. (2020). Physical and Biological Controls of the Drake Passage pCO2 Variability. *Global Biogeochemical Cycles*, *34*(9), e2020GB006644. http://doi.org/10.1029/2020GB006644

Jiang, C., Gille, S. T., Sprintall, J., & Sweeney, C. (2014). Drake Passage Oceanic pCO 2: Evaluating CMIP5 Coupled Carbon–Climate Models Using in situ Observations. *Journal of Climate*, *27*(1), 76–100. http://doi.org/10.1175/JCLI-D-12-00571.1

Johnson, G. C., & Bryden, H. L. (1989). On the size of the Antarctic Circumpolar Current. http://doi.org/10.1016/0198-0149(89)90017-4

Kanamitsu, M., Ebisuzaki, W., Woollen, J., Yang, S.-K., Hnilo, J. J., Fiorino, M., & Potter, G. L. (2002). NCEP–DOE AMIP-II Reanalysis (R-2). *Bulletin of the American Meteorological Society*, *83*(11), 1631–1644. http://doi.org/10.1175/BAMS-83-11-1631

Khatiwala, S., Primeau, F., & Hall, T. (2009). Reconstruction of the history of anthropogenic CO2 concentrations in the ocean. *Nature*, 1–5. http://doi.org/10.1038/nature08526

Landschützer, P., N. Gruber and D.C.E. Bakker (2020). An observation-based global monthly gridded sea surface pCO2 and air-sea CO2 flux product from 1982 onward and its monthly climatology (NCEI Accession 0160558). Version 6.6. NOAA National Centers for Environmental Information. Dataset.

Landschutzer, P., Gruber, N., & Bakker, C. E. (2016). Decadal variations and trends of the global ocean carbon sink. *Global Biogeochemical Cycles*, (30), 1396–1417. http://doi.org/10.1002/(ISSN)1944-9224

Landschutzer, P., Gruber, N., Bakker, D. C. E., & Schuster, U. (2014). Recent variability of the global ocean carbon sink. *Global Biogeochemical Cycles*, *28*(9), 927–949. http://doi.org/10.1002/2014GB004853

Large, W. G., McWilliams, J. C., & Doney, S. C. (1994). Oceanic vertical mixing: a review and a model with a nonlocal boundary layer parameterization. *Rev. Geophysics*, *32*(4), 363–403.

Marshall, J., & Radko, T. (2003). Residual-mean solutions for the Antarctic Circumpolar Current and its associated overturning circulation. *Journal of Physical Oceanography*, *33*(11), 2341–2354. http://doi.org/10.1175/1520-0485(2003)033<2341:RSFTAC>2.0.CO;2

Marshall, J., & Speer, K. (2012). Closure of the meridional overturning circulation through Southern Ocean upwelling. *Nature Geoscience*, 1–10. http://doi.org/10.1038/ngeo1391

Mongwe, N. P., Chang, N., & Monteiro, P. M. S. (2016). The seasonal cycle as a mode to diagnose biases in modelled CO2 fluxes in the Southern Ocean. *Ocean Modelling*, *106*(C), 90–103. http://doi.org/10.1016/j.ocemod.2016.09.006

Pham, A. L. D., & Ito, T. (2021). Anthropogenic Iron Deposition Alters the Ecosystem and Carbon Balance of the Indian Ocean Over a Centennial Timescale. *Journal of Geophysical Research: Oceans*, *126*(2), e2020JC016475. http://doi.org/10.1029/2020JC016475

Redi, M. H. (1982). Oceanic Isopycnal Mixing by Coordinate Rotation. *Journal of Physical Oceanography*, *12*(10), 1154–1158. http://doi.org/10.1175/1520-0485(1982)012<1154:OIMBCR>2.0.CO;2

Tagliabue, A., Williams, R. G., Rogan, N., Achterberg, E. P., & Boyd, P. W. (2014). A ventilation-based framework to explain the regeneration-scavenging balance of iron in the ocean, 1–11. http://doi.org/10.1002/(ISSN)1944‐8007

Toggweiler, J. R., & Russell, J. (2008). Ocean circulation in a warming climate. *Nature*, *451*(7176), 286–288. http://doi.org/10.1038/nature06590

Uchida, T., Balwada, D., Abernathey, R. P., McKinley, G. A., Smith, S. K., & Levy, M. (2020). Vertical eddy iron fluxes support primary production in the open Southern Ocean. *Nature Communications*, 1–8. http://doi.org/10.1038/s41467-020-14955-0

Verdy, A., & Mazloff, M. R. (2017). A data assimilating model for estimating Southern Ocean biogeochemistry. *Journal of Geophysical Research: Oceans*, *122*(9), 6968–6988. http://doi.org/10.1002/2016JC012650